Soft Matter

RSC Publishing

PAPER

View Article Online
View Journal | View Issue

Cite this: *Soft Matter*, 2013, **9**, 8705

Adhesion behavior of mouse liver cancer cells on nanostructured superhydrophobic and superhydrophilic surfaces

Tae-Jun Ko,[ab] Eunkyung Kim,[c] So Nagashima,[a] Kyu Hwan Oh,[b] Kwang-Ryeol Lee,[a] Soyoun Kim[c] and Myoung-Woon Moon*[a]

The control of cancer cell adhesion behavior on certain surfaces has been widely studied in recent years to enhance cell adhesion, which is required for bio-sensing, implant biomaterials, or to prevent infections from bacteria or germs. In addition, it helps to preserve the original functions of medical devices such as implants, catheters, injection syringes, and vascular stents. In this study, we explored the behavior of mouse liver cancer cells on nanostructured surfaces in extreme wetting conditions of a superhydrophobic or superhydrophilic nature. Oxygen plasma treatment of polymeric surfaces induced the formation of nanostructures such as bumps or hairs with various aspect ratios, which is defined as the height to diameter ratio. A superhydrophobic surface with a contact angle (CA) of 161.1° was obtained through the hydrophobic coating of a nanostructured surface with a high aspect ratio of 25.8. On the other hand, an opposite extreme wetting surface with a superhydrophilic nature with a CA of 1.7° was obtained through the hydrophilic coating of the same structured surface. The mouse liver cancer cells significantly proliferated on a mild hydrophilic surface with a low aspect ratio nanostructure due to the mild roughness and improvements of mechanical anchoring. However, the superhydrophilic surface with a high aspect ratio nanostructure (*i.e.*, hair shaped) suppressed the growth of the cancer cells due to the limited number of sites for focal adhesion, which restricted the adhesion of cancer cells and resulted in a decrease in the cell-covered area. The superhydrophobic nanostructured surface with a high aspect ratio further restricted the adhesion and growth of the cancer cells; the cell activity was extremely suppressed and the spherical shape of the cancer cells was maintained. Thus, this simple method for fabricating nanostructured surfaces with various wetting conditions might be useful for producing biomedical devices such as stents, implants, drug delivery devices, and detection and/or sensing devices for cancer cells.

Received 25th April 2013
Accepted 15th July 2013

DOI: 10.1039/c3sm51147b

www.rsc.org/softmatter

1 Introduction

The control of cell adhesion on functional surfaces has been widely studied in recent years to enhance the cell adhesion required for bio-sensing[1] and the implanting of biomaterials.[2] However, other functions may be required to prohibit the adhesion of pathogenic bacteria, germs, and cancer cells on surfaces to prevent infection as well as to preserve the original function of medical devices such as implants, catheters, injection syringes, and vascular stents.[3] The nature of the cell adhesion to biomaterials is known to depend on surface characteristics such as the surface energy and morphology.[2,4–8] Thus, through modifying surface properties, it is possible to control not only cell adhesion but also the proliferation and differentiation of the adherent cells. Cell adhesion behavior was recently found to depend on the aspect ratio of the surface, which is defined as the ratio of the width or diameter to the length or height of nanostructures on the surface. A low aspect ratio would enhance cell adhesion because of a mechanical anchoring effect while a high aspect ratio would repel cells by lowering the focal area for adhesion.[8,9]

Recently, cell adhesion behavior has been examined on nano-featured surfaces with various morphologies such as nanopillars,[5,10,11] nanobumps,[12–14] or nanopores[6,8] created using nanoimprinting,[5] e-beam lithography,[15] optical lithography,[16] block-copolymer lithography,[17] and chemical or plasma etching techniques.[18] A recent review of surface nanostructuring indicated that plasma treatment or etching can be used to modify biomaterials as they can easily be carried out at low

[a]*Institute for Multidisciplinary Convergence of Matter, Korea Institute of Science and Technology, 136-791 Seoul, Republic of Korea. E-mail: mwmoon@kist.re.kr; Fax: +82 2 958 5509; Tel: +82 2 958 5487*

[b]*Department of Materials Science and Engineering, Seoul National University, 151-742 Seoul, Republic of Korea*

[c]*Department of Biomedical Engineering, Dongguk University, 100-715 Seoul, Republic of Korea*

temperatures and are biocompatible.[19,20] In particular, polymeric surfaces can be altered by the plasma treatment, which controls the surface energy and morphological features.[21,22] Furthermore, superhydrophilic (a water contacting angle (CA) of less than 10°) or superhydrophobic (a CA of over 150°) surfaces can be achieved or even enhanced by combining nanostructuring and surface coating with materials with a specific surface energy.[3,23]

Hydrophilic or superhydrophilic surfaces induced by oxygen or argon plasma are used to improve cell adhesion,[24,25] whereas hydrophobic or superhydrophobic surfaces are used for anti-cell adhesion.[4] Aggressive cells, such as cancer cells, may grow in a disordered way and continue to proliferate even in a crowded environment.[26] In addition, these cells can divide infinitely and therefore easily migrate to other healthy organs.[27] In particular, metastasis, which is the spread of cancer from one organ to another to form new tumors in a non-adjacent organ, may be prevented by controlling the adhesion of cancer cells. Additionally, the detection of cancer on a specifically functionalized surface at an early stage before it is widely spread might offer sufficient time for the cancer to be treated successfully by surgery, which would result in the patient being cured.[27] Therefore, it is important to control the adhesion and growth of cancer cells to prevent the migration of cancer cells and/or increase their efficient detection. However, the adhesion of cancer cells, such as liver cancer cells, to extreme wetting nanostructured surfaces has not yet been studied.

In this work, we explored the behavior of cancer cells on wettability controlled surfaces of a superhydrophobic or superhydrophilic nature. Mouse liver cancer cells were grown on extreme wetting surfaces with controlled surface nanostructures and surface coating materials with different surface energies. The nanostructures on the polymers, which exhibited various aspect ratios, were fabricated by oxygen plasma ion etching. In addition, the surface morphology of the nanostructures, which varied from nanobump to nanohair, was controlled during the plasma treatment. Subsequently, the deposition of Si-DLC (diamond-like carbon) with oxygen plasma treatment or the deposition of SiO_x-DLC was performed to render the nanostructured surfaces superhydrophilic or superhydrophobic, respectively.

We chose mouse liver cancer cells as the research target as they are similar to their human counterparts.[28] Liver cancer is one of the most prevalent and lethal cancers due to its high mortality rate.[29] Therefore, it is important to control the adhesion of cancer cells to increase the efficiency of the diagnosis and/or prevent metastasis. We found that cancer cells strongly proliferate on a mildly hydrophilic surface with a mild roughness, as shown in Fig. 1a. Note that the total amount of cancer cells grown on the superhydrophobic or superhydrophilic surfaces is larger than that of non-cancerous normal cells because cancer cells are able to grow rapidly and divide before they fully mature, while non-cancerous normal cells stop growing when they get a signal from other nearby cells.[26,30] However, a significantly lower cell density was found on the superhydrophilic surfaces with nanohair morphology and a higher aspect ratio, as shown in Fig. 1b. On the superhydrophobic nanostructured surfaces, cell growth was significantly restricted, cell activity was extremely suppressed, and the spherical shape of the cancer cells was maintained, as shown in Fig. 1c. The adhesion behavior of mouse liver cancer cells was investigated on both extreme wetting surfaces with a scanning electron microscope (SEM) and image processing using an optical microscope. The morphology of the nanostructured surface was characterized using a SEM and an atomic force microscope (AFM), and the wettability of the surface was characterized by measuring the water CA.

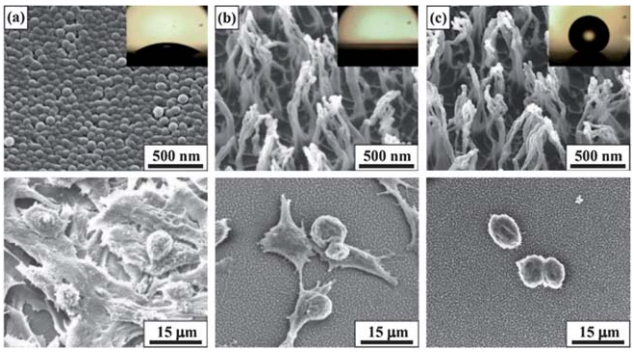

Fig. 1 SEM images of (top) plasma-treated surfaces and (bottom) the adhesion behavior of mouse liver cancer cells on (a) a hydrophilic surface after 1 min of oxygen plasma etching, (b) a hydrophilic surface after 30 min of oxygen plasma etching, and (c) a hydrophobic surface after 30 min of oxygen plasma etching. The insets show the corresponding optical images of water droplets on each surface.

2 Experimental

Sample preparation

We chose a commercially available polyethylene terephthalate (PET, SK chemical, Rep. Korea) as the substrate. This material was cut into sections of $50 \times 30 \times 0.2$ mm^3. The oxygen plasma etching technique using a radio-frequency plasma-enhanced chemical vapor deposition (rf-PECVD) system was employed to fabricate the nanostructures. The various morphologies of these nanostructures, which ranged from nanobump to nanohair, were controlled by the duration of the plasma etching (1 to 30 min). The gas pressure and the bias voltage were maintained at 20 mTorr and −400 V, respectively.

The surface energy of each sample was tuned by choosing coatings with different surface energies. A DLC thin film with incorporated Si (denoted Si-DLC) was deposited with a mixed precursor of benzene and diluted silane ($SiH_4 : H_2$, 10 : 90) gases at a ratio of 97.5 : 2.5. The Si-DLC surfaces that were subsequently subjected to oxygen plasma treatment for 30 s become hydrophilic, and this feature lasted even after immersion in water for more than 2 weeks.[31] Additionally, a DLC film with incorporated SiO_x (denoted SiO_x-DLC), which exhibited a surface energy of 24.2 mN m^{-1} with hexamethyldisiloxane (HMDSO) as a precursor, was employed to increase the hydrophobicity of the surface.[21] The gas pressure and the bias voltage used in both coating methods were maintained at 10 mTorr and −400 V, respectively.

Morphology analysis

The morphology of the polymer surfaces before and after oxygen plasma etching was observed with a scanning electron microscope (SEM, FEI, Nova NanoSEM 200) at a 10 kV electron acceleration voltage. The roughness of the surface was measured in at least five different spots in an area of 10 × 10 μm^2 using an atomic force microscope (AFM, Park systems Co., XE-70) in the non-contact mode.

Contact angle and contact angle hysteresis

The wettability of the pristine and modified PET samples was characterized by measuring the water contact angle (CA) and contact angle hysteresis (CAH) of deionized (DI) water through a sessile drop test. To measure the CA, approximately 5 μL droplets were gently deposited on the PET surfaces using a microsyringe. The CA values were measured using a goniometer (Rame-Hart, Mountain Lakes, NJ) in ambient air at 20 °C with a relative humidity of 20–35%. The CA was measured in at least five different spots on each sample, and the average CA value was calculated. The CAH was calculated as the difference between the advancing CA and receding CA. The advancing CA was measured during supply of the water on the deposited droplet and the receding CA was measured during removal of the deposited water droplet.

Cell culture and measurement of adhered cell-covered area

Mouse liver cancer cells (BNL 1ME A.7R.1, ATCC) were cultured in Dulbecco's modified Eagle's medium (DMEM, ATCC) supplemented with 10% fetal bovine serum (FBS, Invitrogen), and penicillin/streptomycin (100 U ml^{-1}, Invitrogen). A cell density of 5 × 10^4 cells per ml was seeded on 1.0 cm^2 of the polymeric surface, which was divided by sticky slides into 8 wells (ibidi GmbH, Munich, Germany). The cells were incubated for 3 days at 37 °C in a humidified 5% CO_2 incubator. The cultured cells were observed through phase-contrast microscopy (BX-71, Olympus) in at least 8 areas for each sample. The acquired images were analyzed to quantify the ratio of the cell-covered area with ImageJ software (Version 1.46, NIH, Bethesda, MD).

Observation of cell adhesion behavior

The morphology of the adherent cells was observed under SEM. Prior to the SEM observations, the medium was removed and the cells were washed with phosphate-buffered saline (PBS, pH 7.4, Invitrogen). Next, the cells were incubated with paraformaldehyde (4% PFA in PBS) for 1 h and then with osmium tetroxide (2% OsO_4 in PBS) for 2 h. After incubation, the cells were dehydrated using multistage ethanol solutions (30, 50, 80, and 99%). The cells were then fixed using hexamethyldisilazane for 20 min and dried in air for 24 h to remove the solution.

3 Results and discussion

Surface morphology

The PET samples exposed to oxygen plasma were found to have nanostructures with various aspect ratios depending on the exposure duration, as shown in Fig. 2. As the duration of the plasma exposure was increased from 1 to 30 min, the height of the nanostructures significantly increased from 67 to 884 nm, whereas the diameter was maintained at approximately 40 nm. As shown in Table 1, the aspect ratio of the nanostructures linearly increased to 25.8. It was also noted that the nanohair structures started aggregating due to the van der Waals forces between these structures obtained after 30 min of plasma exposure. The mechanism of nanostructure formation has not yet been investigated. Several hypotheses have been reported explaining the formation of nanostructures on polymeric surfaces by oxygen plasma treatment. The different etching rates of the crystalline or amorphous phase in PET have been found to cause patterns with a high aspect ratio.[32] In addition to this mechanism, recent reports have shown that the deposition of metal particles from the plasma chamber plays a certain role in the resistance of the polymeric surface against etching by oxygen plasma, *i.e.*, these particles act as local etching inhibitors.[22,33]

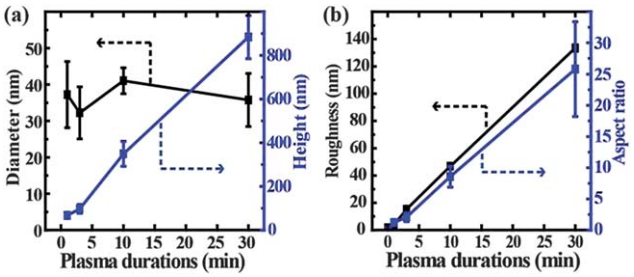

Fig. 2 (a) Graph of the diameter and height of the nanostructure as a function of the plasma treatment duration. (b) Graph of the roughness of the surface and the aspect ratio of the nanostructure as a function of the plasma treatment duration.

Wettability

All of the sample conditions are listed in Table 2 in abbreviated forms, such as 0PHI (only hydrophilic coating) or 30PHO (hydrophobic coating after 30 min of oxygen plasma etching). The wettability of the plasma-treated PET samples was explored by measuring the static CAs of the sessile water drops, as shown in Fig. 3. The CA of the pristine PET sample was measured to be 61.1°. In contrast, the CA of the 0PHI sample decreased to 33.5° due to the hydrophilic coating while that of the 0PHO sample increased to 89.8°, which is an intrinsic water CA for the SiO_x-DLC coating. It is well known that the deposition of the

Table 1 Morphologies of the oxygen plasma-treated PET surfaces with respect to the oxygen plasma duration

O_2 plasma duration (min)	Roughness (R_{rms}, nm)	Diameter (nm)	Height (nm)	Aspect ratio
0	1.8	—	—	—
1	3.9	37.2	67.0	1.9
3	15.3	32.2	97.2	3.2
10	46.8	41.0	349.2	8.6
30	133.4	35.8	884.2	25.8

Table 2 Surface properties of the plasma-treated samples with different surface energies

Sample	O_2 plasma duration (min)	Aspect ratio	CA (degree)	CAH (degree)
Pristine	—	—	61.1 ± 0.8	28.3 ± 0.5
0PHI	—	—	33.5 ± 3.2	27.5 ± 3.2
1PHI	1	1.9	25.9 ± 2.6	22.4 ± 4.6
3PHI	3	3.2	6.6 ± 1.1	4.6 ± 2.1
10PHI	10	8.6	1.8 ± 0.3	0.4 ± 0.2
30PHI	30	25.8	1.7 ± 0.4	0.2 ± 0.1
0PHO	—	—	89.8 ± 1.9	22.4 ± 4.6
1PHO	1	1.9	91.4 ± 3.1	27.3 ± 3.4
3PHO	3	3.2	104.3 ± 2.3	29.8 ± 3.7
10PHO	10	8.6	157.2 ± 3.6	3.4 ± 1.8
30PHO	30	25.8	161.1 ± 2.8	2.2 ± 1.1

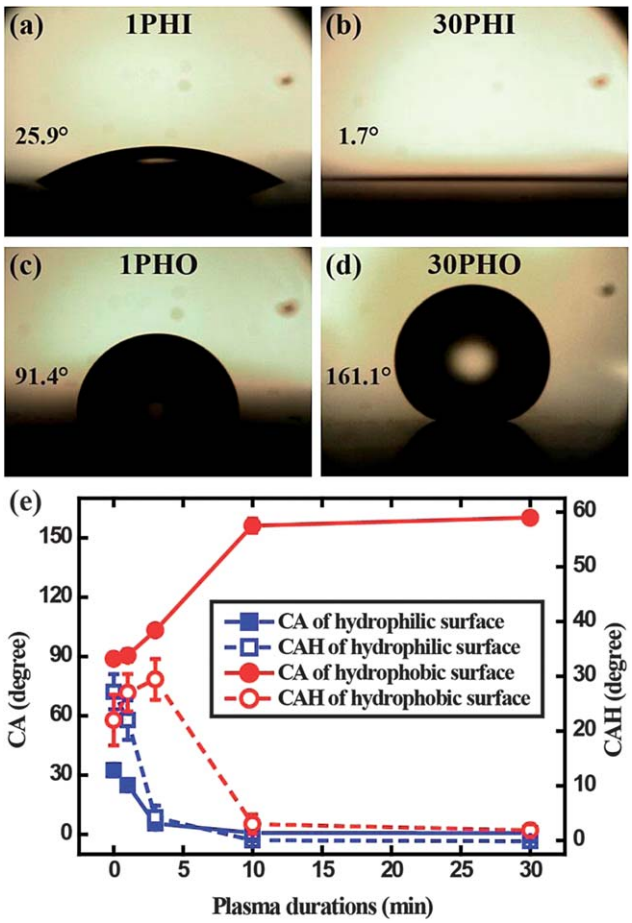

Fig. 3 Images of sessile water droplets deposited on the (a) 1PHI, (b) 30PHI, (c) 1PHO, and (d) 30PHO samples. (e) Graph of the CA of the water droplets as a function of the oxygen plasma treatment duration and the hydrophilic/hydrophobic coating.

hydrophilic/hydrophobic coatings on nanostructured surfaces enhances the hydrophilicity and hydrophobicity of the surfaces to superhydrophilicity and superhydrophobicity, respectively.[34] After nanostructuring through oxygen plasma etching and subsequent hydrophilic treatment, the CA of the 30PHI sample decreased to 1.7° while the CA of the 30PHO sample increased to 161.1°. As the oxygen plasma exposure duration was increased, the aspect ratio of the nanostructures increased. As a result, air traps were formed between the nanostructures, and these air traps have an important role in achieving superhydrophobicity.[34,35]

Cell adhesion behavior

We conducted SEM observations on four samples to investigate the effects of roughness and surface energy on the adhesion behavior of cancer cells. The mouse liver cancer cells were cultured on the 1PHI, 30PHI, 1PHO, and 30PHO samples for 3 days, and the final morphologies were explored using low and high magnification SEM images as shown in Fig. 4. The number of adherent cells in the 1PHI sample, which grew in multiple layers, was high compared to the other three samples. As we mentioned before, cancer cells grow and divide well even in crowded environments to form multiple layers. The cells spread well on the surface and exhibited a flat and polygonal shape as well as having many filopodia stretched out to form mechanical anchors on the mildly plasma-treated substrate as shown in Fig. 4b. In contrast, the analysis of the 30PHI sample showed filopodia that were restricted and extended in one direction only along the top of the nanohairs with a small number of protrusions in the top and tilt view images. Thus, in the 30PHI case the width of the filopodia was shorter and the length was longer than those observed in the 1PHI sample, as shown in Fig. 4b. Due to the limited contact sites on the hair-like nanostructured surface with a high aspect ratio, it was found that the cells maintained a relatively hemispherical shape as shown in Fig. 4c, and the number of adherent cells on the 30PHI sample was lower. In the case of the hydrophobic coated surface, the number of adherent cells on 1PHO was smaller than that on 1PHI, although the adherent cells on 1PHO spread well and exhibited a flat-polygon shape. The hydrophobic coating is considered to prevent or delay the initial cell adhesion, but cells spread well in a flat shape after they were deposited on the substrate due to the large number of focal sites. However, the anti-adhesion behavior was greatly enhanced on the superhydrophobic surface as shown in Fig. 4a of the 30PHO sample. Because of the low wettability of the hydrophobic film and the higher water CA, this surface interacts less with the cells in the medium. The superhydrophobic surface with a high aspect ratio nanostructure favors the formation of air traps between the nanostructures, which prevent the protein layer from making contact with the sides of the hairs and the bottom surfaces and consequently restricts cell adhesion.[3] Note that the entire surface of the nanohairs in the 30PHI sample would be covered with an extracellular protein layer as shown in Fig. 4b, which plays an important role in the adhesion of cells to the target surface. As a result, the cells on the 30PHO sample maintained a spherical shape, which indicates that these did not grow due to the small degree of filopodia spreading. The adherent cells tended to aggregate on top of the nanostructure, resulting in the cells adhering to the surface in a cooperative manner due to the weak adhesion between the cancer cells and

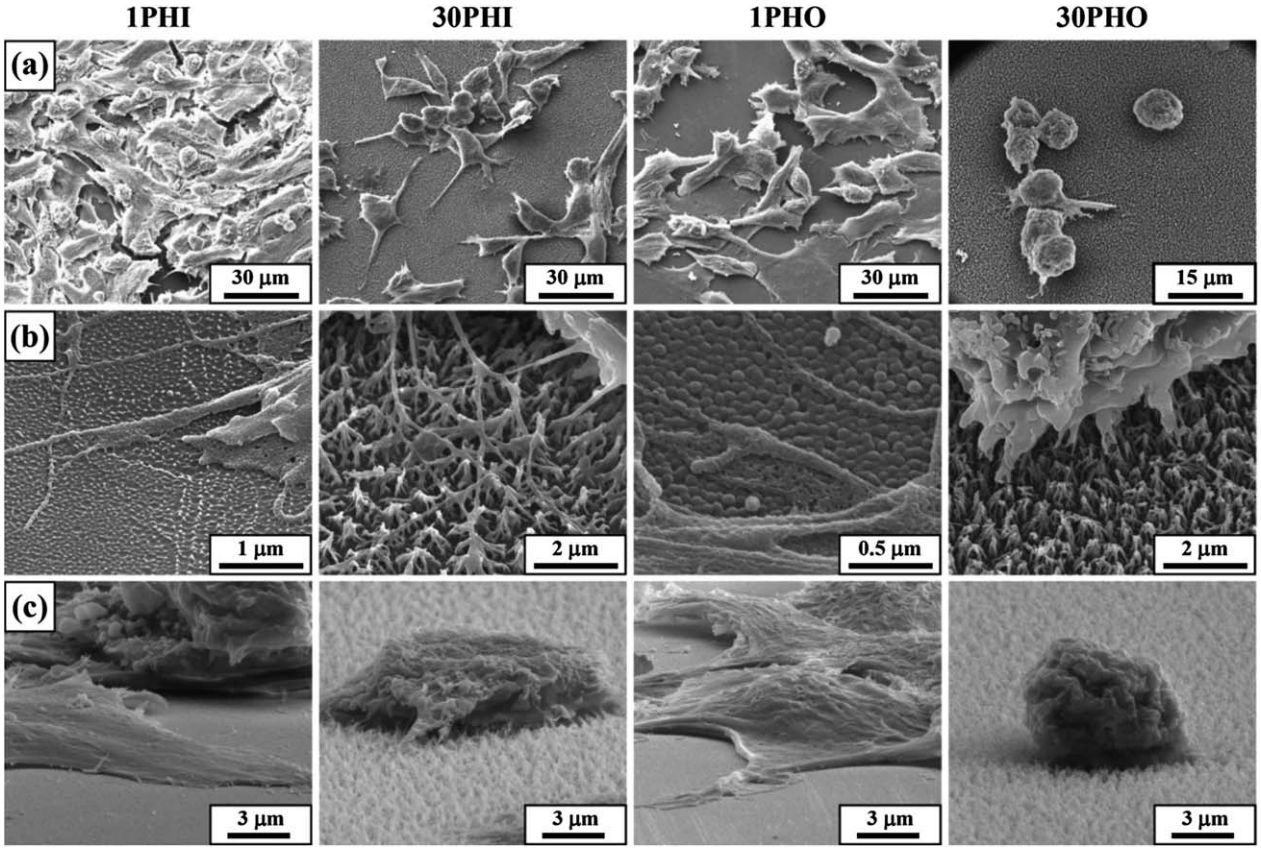

Fig. 4 SEM images of the adhesion behavior of mouse liver cancer cells on the 1PHI, 30PHI, 1PHO, and 30PHO samples; 30° tilt view with (a) low magnification, (b) high magnification, and (c) 60° tilt view of each sample.

the top of the nanohairs.[5,36,37] Also, cancer cells on the super-hydrophobic 30PHO surface have an abnormal appearance of a highly wrinkled spherical shape as shown in Fig. 4c. This abnormal configuration of the cells has been known to be a signal of apoptosis, or programmed cell death in non-cancerous cells due to the hindering of cell activity by the low level of adhesive interaction.[12] Even though, the activity of cancer cells grown on the 30PHO surface is shown to be lower on this nanostructured surface than on the surface of the 1PHO sample, it is hard to conclude that the mouse liver cancer cells are in the process of apoptosis from this analysis, which will be confirmed in future works.

Density of adherent cells

The bio-adhesion mechanism has been investigated for several decades. The literature indicates that bio-adhesion occurs in the following steps: cell deposition, attachment of a protein layer, and proliferation.[2] The optical microscope images of the cells cultured for 3 days on surfaces modified under different conditions were used for quantitative analysis by measuring the ratio of the cell-covered area (the area covered by cells divided by the projected area), as shown in Fig. 5a. In the case of a pristine surface with mild hydrophilicity, cancer cells were deposited well within 1 day of culture and began to spread within 2 days, eventually covering 23.5% of the area with cancer cells. After hydrophilic coating, the cancer cells were observed to have spread in less than 1 day. The surface area covered by cells in the 0PHI sample increased to 64% due to the hydrophilic coating. All of the samples with a hydrophilic coating exhibited a higher ratio of cell-covered area than the pristine sample. The 1PHI nanostructured samples with a low aspect ratio exhibited a higher ratio of cell-covered area than those obtained on hydrophilic coated samples with a longer plasma treatment of 3, 10 and 30 min. Because the cells can follow the topography of the substrate, the flexibility of the cells along a surface with a mild roughness can enhance mechanical anchoring through the formation of focal adhesions.[3,38] According to previous studies, this enhancement has a strong correlation with the aspect ratio of the nanostructure.[8,9] In our case, this enhancement was maintained for an oxygen plasma duration of 1 min, or equivalently, an aspect ratio of 1.9. As the aspect ratio of the nanostructures increased after more than 1 min of oxygen plasma etching, the ability of the cancer cells to adhere to the surface was restricted, which resulted in a reduced ratio of the cell-covered area, as shown in Fig. 5b. In the case of the hydrophobic coating, the cell-covered area ratio of the 0PHO sample was 13.4%, which was smaller than that of the pristine sample. Due to the low surface energy not many of the proteins which help the adherence of cancer cells to a surface were deposited; thus, the strength of the cell adhesion was lower than that found on a hydrophilic surface. Furthermore, the cells

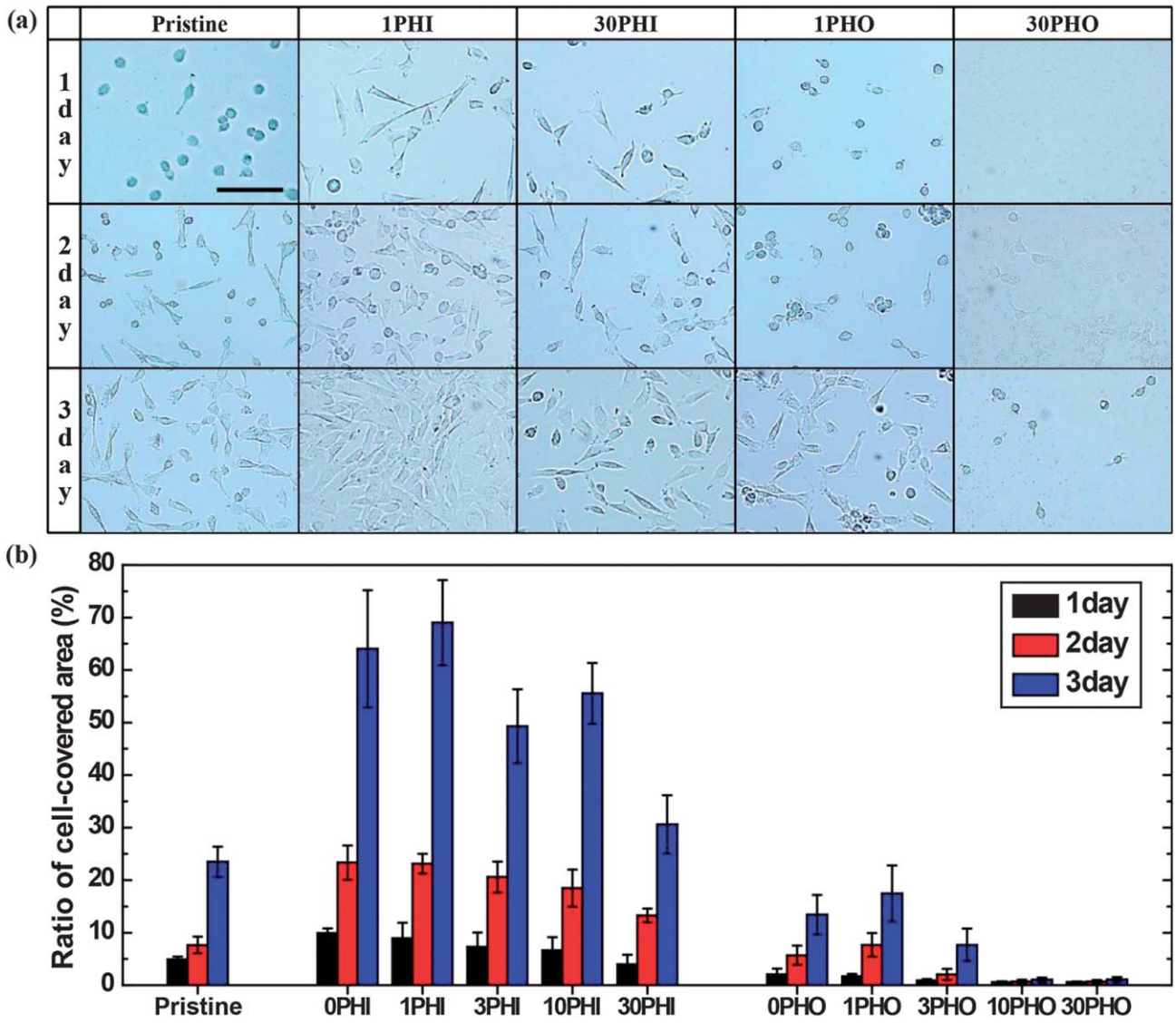

Fig. 5 (a) Optical microscope images of cells cultured for 3 days on PET surfaces modified with different oxygen plasma durations (1 or 30 min) and coating conditions (hydrophilic or hydrophobic). The scale bar is 100 μm. (b) The ratio of the cell-covered area (%) of pristine, hydrophilic-coated, and hydrophobic-coated PET samples with different oxygen plasma treatments after 1–3 days of culture.

did not adhere well to the surface of the 30PHO sample and remained slightly spread-out with a spherical shape even after 3 days of culture. As a result, the cell-covered area ratio decreased to 0.5%, which is much smaller than that obtained on the pristine surface. As mentioned before, this anti-adhesion behavior originated from the reduced focal adhesion and the decreased adsorption of a protein layer.

4 Conclusion

Wettability tuned surfaces with nanostructuring and subsequent coating with materials with different surface energies were explored to control the adhesion and growth behavior of cancer cells. The oxygen plasma treatment of the polymeric surface provided nanostructures, such as bump or hair, with various aspect ratios. This increased the aspect ratios up to 25.8 with an increase in the plasma duration up to 30 min. The wettability of the surface was easily tuned by hydrophilic and hydrophobic material coatings after nanostructuring, which resulted in the formation of superhydrophilic and superhydrophobic surfaces with contact angles of 1.7° and 161.1°, respectively.

The behavior of mouse liver cancer cells on the nanostructured surfaces with extreme wetting of a superhydrophobic or superhydrophilic nature was explored. It was found that the liver cancer cells significantly proliferated on mildly hydrophilic surfaces with a low aspect ratio nanostructure due to enhanced mechanical anchoring. However, the superhydrophilic surfaces with a high aspect ratio nanostructure, *i.e.*, hair shaped, suppressed the growth of the cancer cells due to the limited sites for focal adhesion, which restricted the adhesion of cancer cells and resulted in a decrease in the cell-covered area. A superhydrophobic surface with a high aspect ratio further restricted

the adhesion and growth of the cancer cells; the cell activity was extremely suppressed and the spherical shape of the cancer cells was maintained. This result presents the possibility that morphology and surface energy control of substrates could be used to suppress cancer cells differentiating and proliferating,[39,40] which may be carefully analyzed in future work.

Thus, this simple method of fabricating nanostructured surfaces with tuned extreme wetting conditions is a promising approach for controlling (either suppression or enhancement) the adhesion of cancer cells, which might be applicable for biomedical devices such as stents, implants, drug delivery devices, and detection and sensing devices for cancer cells.

Acknowledgements

This work was supported by the KIST internal project, the Global Excellent Technology Innovation R&D Program of the Ministry of Knowledge Economy (MKE), the Republic of Korea, and Project no. 10040003 funded by the MKE. This work was also funded by the Ministry of Education, Science, and Technology (R11-2005-065, OKH).

Notes and references

1 Y. Wan, M. A. Mahmood, N. Li, P. B. Allen, Y. T. Kim, R. Bachoo, A. D. Ellington and S. M. Iqbal, *Cancer*, 2012, **118**, 1145–1154.
2 G. Legeay and F. Poncin-Epaillard, in *Adhesion*, Wiley-VCH Verlag GmbH & Co. KGaA, 2006, pp. 175–188.
3 G. Legeay, A. Coudreuse, F. Poncin-Epaillard, J. M. Herry and M. N. Bellon-Fontaine, *J. Adhes. Sci. Technol.*, 2010, **24**, 2301–2322.
4 T. Ishizaki, N. Saito and O. Takai, *Langmuir*, 2010, **26**, 8147–8154.
5 H. Walter, S. C. Adam, M. Danielle, A. Mukti and J. L. Kevin, *Nanotechnology*, 2010, **21**, 385301.
6 L. Richert, F. Vetrone, J. H. Yi, S. F. Zalzal, J. D. Wuest, F. Rosei and A. Nanci, *Adv. Mater.*, 2008, **20**, 1488–1492.
7 Y. Rahmawan, K. J. Jang, M. W. Moon, K. R. Lee and K. Y. Suh, *BioChip J.*, 2009, **3**, 143–150.
8 S. H. Chung, S. J. Son and J. Min, *Nanotechnology*, 2010, **21**, 125104.
9 A. S. Crouch, D. Miller, K. J. Luebke and W. Hu, *Biomaterials*, 2009, **30**, 1560–1567.
10 C. H. Choi, S. H. Hagvall, B. M. Wu, J. C. Dunn, R. E. Beygui and C. J. Kim, *Biomaterials*, 2007, **28**, 1672–1679.
11 P. Kim, D. H. Kim, B. Kim, S. K. Choi, S. H. Lee, A. Khademhosseini, R. Langer and K. Y. Suh, *Nanotechnology*, 2005, **16**, 2420–2426.
12 H. A. Pan, Y. C. Hung, C. W. Su, S. M. Tai, C. H. Chen, F. H. Ko and G. Steve Huang, *Nanoscale Res. Lett.*, 2009, **4**, 903–912.
13 E. A. Cavalcanti-Adam, A. Micoulet, J. Blummel, J. Auernheimer, H. Kessler and J. P. Spatz, *Eur. J. Cell Biol.*, 2006, **85**, 219–224.
14 R. Di Mundo, R. Gristina, E. Sardella, F. Intranuovo, M. Nardulli, A. Milella, F. Palumbo, R. d'Agostino and P. Favia, *Plasma Processes Polym.*, 2010, **7**, 212–223.
15 N. Q. Balaban, U. S. Schwarz, D. Riveline, P. Goichberg, G. Tzur, I. Sabanay, D. Mahalu, S. Safran, A. Bershadsky, L. Addadi and B. Geiger, *Nat. Cell Biol.*, 2001, **3**, 466–472.
16 A. Accardo, F. Gentile, F. Mecarini, F. De Angelis, M. Burghammer, E. Di Fabrizio and C. Riekel, *Microelectron. Eng.*, 2011, **88**, 1660–1663.
17 J. P. Spatz and B. Geiger, *Methods Cell Biol.*, 2007, **83**, 89–111.
18 J. M. Łopacińska, C. Grădinaru, R. Wierzbicki, C. Købler, M. S. Schmidt, M. T. Madsen, M. Skolimowski, M. Dufva, H. Flyvbjerg and K. Mølhave, *Nanoscale*, 2012, **4**, 3739–3745.
19 P. A. Ramires, L. Mirenghi, A. R. Romano, F. Palumbo and G. Nicolardi, *J. Biomed. Mater. Res.*, 2000, **51**, 535–539.
20 M. Chen, P. O. Zamora, P. Som, L. A. Pena and S. Osaki, *J. Biomater. Sci., Polym. Ed.*, 2003, **14**, 917–935.
21 B. S. Shin, K. R. Lee, M. W. Moon and H. Y. Kim, *Soft Matter*, 2012, **8**, 1817–1823.
22 K. Tsougeni, N. Vourdas, A. Tserepi, E. Gogolides and C. Cardinaud, *Langmuir*, 2009, **25**, 11748–11759.
23 W. J. Ma, A. J. Ruys, R. S. Mason, P. J. Martin, A. Bendavid, Z. Liu, M. Ionescu and H. Zreiqat, *Biomaterials*, 2007, **28**, 1620–1628.
24 K. E. Schmalenberg, H. M. Buettner and K. E. Uhrich, *Biomaterials*, 2004, **25**, 1851–1857.
25 S. Tajima, J. S. Chu, S. Li and K. Komvopoulos, *J. Biomed. Mater. Res., Part A*, 2008, **84**, 828–836.
26 W. H. Clark, Jr, *Acta Oncol.*, 1995, **34**, 3–21.
27 A. F. Chambers, A. C. Groom and I. C. MacDonald, *Nat. Rev. Cancer*, 2002, **2**, 563–572.
28 M. W. Leenders, M. W. Nijkamp and I. H. Borel Rinkes, *World J. Gastroenterol.*, 2008, **14**, 6915–6923.
29 S. Ma, K. W. Chan, L. Hu, T. K. Lee, J. Y. Wo, I. O. Ng, B. J. Zheng and X. Y. Guan, *Gastroenterology*, 2007, **132**, 2542–2556.
30 R. J. DeBerardinis, J. J. Lum, G. Hatzivassiliou and C. B. Thompson, *Cell Metab.*, 2008, **7**, 11–20.
31 J. W. Yi, M. W. Moon, S. F. Ahmed, H. Kim, T. G. Cha, H. Y. Kim, S. S. Kim and K. R. Lee, *Langmuir*, 2010, **26**, 17203–17209.
32 Y. J. Hwang, S. Matthews, M. McCord and M. Bourham, *J. Electrochem. Soc.*, 2004, **151**, C495–C501.
33 G. Evangelos, C. Vassilios, K. George, K. Dimitrios, T. Katerina, B. George, V. Marilena and T. Angeliki, *J. Phys. D: Appl. Phys.*, 2011, **44**, 174021.
34 D. Quere, in *Annual Review of Materials Research*, Annual Reviews, Palo Alto, 2008, vol. 38, pp. 71–99.
35 A. Lafuma and D. Quere, *Nat. Mater.*, 2003, **2**, 457–460.
36 C. C. Berry, A. S. Curtis, R. O. Oreffo, H. Agheli and D. S. Sutherland, *IEEE Trans. NanoBiosci.*, 2007, **6**, 201–209.
37 C. D. W. Wilkinson, A. S. G. Curtis and J. Crossan, *J. Vac. Sci. Technol., B*, 1998, **16**, 3132–3136.
38 Y. Wan, Y. Wang, Z. Liu, X. Qu, B. Han, J. Bei and S. Wang, *Biomaterials*, 2005, **26**, 4453–4459.
39 S. Huang and D. E. Ingber, *Nat. Cell Biol.*, 1999, **1**, E131–E138.
40 S. Huang, C. S. Chen and D. E. Ingber, *Mol. Biol. Cell*, 1998, **9**, 3179–3193.